© 2021. Published by The Company of Biologists Ltd | Journal of Experimental Biology (2021) 224, jeb242508. doi:10.1242/jeb.242508

RESEARCH ARTICLE

Proleg retractor muscles in *Manduca sexta* larvae are segmentally different, suggesting anteroposterior specialization

Anthony E. Scibelli[1,*], Daniel P. Caron[1], Hitoshi Aonuma[2] and Barry A. Trimmer[1]

ABSTRACT

Manduca sexta larvae are an important model system for studying the neuromechanics of soft body locomotion. They climb on plants using the abdominal prolegs to grip and maneuver in any orientation and on different surfaces. The prolegs grip passively with an array of cuticular hooks, and grip release is actively controlled by retractor muscles inserted into the soft planta membrane at the proleg tip. Until now, the principal planta retractor muscles (PPRMs) in each body segment were thought to be a single fiber bundle originating on the lateral body wall. Here, using high resolution X-ray microtomography of intact animals, we show that the PPRM is a more complex muscle consisting of multiple contractile fibers originating at several distinct sites on the proleg. Furthermore, we show that there are segmental differences in the number and size of some of these fiber groups which suggests that the prolegs may operate differently along the anterior–posterior axis.

KEY WORDS: Principal planta retractor muscle, Morphology, Micro-CT, Soft body locomotion

INTRODUCTION

Animal movements depend on a complex interaction between neural commands, muscle function, and the shape and material properties of the body. For animals with stiff skeletons and articulated limbs, the actions of muscles are constrained by joints, and movements can often be predicted by modeling the muscle force–length relationships produced by patterns of neural motor activity (Delp and Loan, 2000; Dembia et al., 2021; Thelen et al., 2003). In contrast, the control of movements by soft animals is much more difficult to predict. They lack defined joints and instead move by deforming limbs, changing the shape of their body and exerting internal hydrostatic or hydraulic forces (Kier, 2012). For such animals, the shape and mechanical properties of soft tissues play a much more significant role in generating and controlling movements (Buschmann and Trimmer, 2017; Hanassy et al., 2015; Levy et al., 2015, 2017; Richter et al., 2015; Sumbre et al., 2005; Trimmer and Lin, 2014; Yekutieli et al., 2005). There are major technical challenges to understanding how the nervous systems of soft animals cope with these increased degrees of freedom. In addition, the three-dimensional interconnected arrangement of muscles in soft animals is complex and often poorly understood, which makes their movements exceedingly difficult to model (Gutfreund et al., 1998; Heckscher et al., 2012; Kier, 1988; Kier and Smith, 1985; Kier and Stella, 2007; Matzner et al., 2000; Nishikawa et al., 1999; Quillin, 1998; Smith and Kier, 1989).

Caterpillars are tractable models for understanding some of these control strategies. They are able to navigate complex and varied environments with a relatively small nervous system, and movements are coordinated by discrete muscles, each controlled by one or occasionally two motoneurons (Taylor and Truman, 1974). Furthermore, the body is propelled by large longitudinal muscles in each abdominal body segment whose activity can be monitored with electromyographic electrodes in freely moving animals (Metallo and Trimmer, 2015; Simon et al., 2010a). In the tobacco hornworm *Manduca sexta*, phasic activation of these muscles produces an anterograde wave of contractions (Trimmer and Issberner, 2007), which, when coupled with controlled gripping (Belanger et al., 2000; Belanger and Trimmer, 2000; Mukherjee et al., 2018) and visceral pistoning (Simon et al., 2010b), moves the caterpillar forward in a steady crawl. Although each body segment undergoes cyclic shortening and re-extension, the timing of substrate grip and release keeps the abdomen in tension so that compressive forces are applied to the substrate; this has been termed the 'environmental skeleton' strategy (Lin and Trimmer, 2010a,b). The longitudinal muscles provide much of the force needed for locomotion, but it is the precise timing of grip and release by the abdominal prolegs that produces a characteristic caterpillar gait (Metallo et al., 2020). Stiff cuticular hooks (crochets) at the tip of the proleg passively grip the substrate when the muscles are relaxed. In response to retractor muscle activation, these crochets release from the substrate (Mukherjee et al., 2018) and the proleg is lifted and carried forward during the swing phase of each step cycle.

The neural activation of proleg retractor muscles has been studied in some detail (Cox, 1989; Weeks and Jacobs, 1987) but relatively little is known about their organization or the mechanical processes leading to crochet retraction. In *Manduca sexta*, two motor units have been identified: a single motoneuron controlling the principal planta retractor muscle (PPRM) (Weeks and Jacobs, 1987), and a pair of indistinguishable neurons controlling the accessory planta retractor muscle (APRM) (Sandstrom and Weeks, 1996) (Fig. 1). Crochet release is initiated by the PPRM and proleg retraction involves continued activity of the PPRM and the recruitment of the APRM (Weeks and Jacobs, 1987). However, because both muscles insert onto soft cuticle, it is hard to predict how the proleg will move in response to different muscle contractions, and invasive monitoring (e.g. electrode insertion) can disrupt normal mechanical processes. What is needed is a computational simulation of the proleg system based on the response properties of the muscle to different patterns of activation, the material properties of the cuticle, internal pressure changes and an accurate structural model of the muscles and proleg.

To date, the morphology of *M. sexta* and other caterpillars has relied on reconstruction from dissected animals flattened in a dish

[1]Tufts University, Department of Biology, 200 Boston Avenue, Suite 2600, Medford, MA 02155, USA. [2]Research Institute for Electronic Science, Hokkaido University, Sapporo, Hokkaido 060-0812, Japan.

*Author for correspondence (scibelli.a@gmail.com)

A.E.S., 0000-0001-9804-5298; D.P.C., 0000-0002-1500-8713; H.A., 0000-0001-8380-1820; B.A.T., 0000-0003-1782-7373

Received 17 March 2021; Accepted 1 June 2021

Journal of Experimental Biology (2021) 224, jeb242508. doi:10.1242/jeb.242508

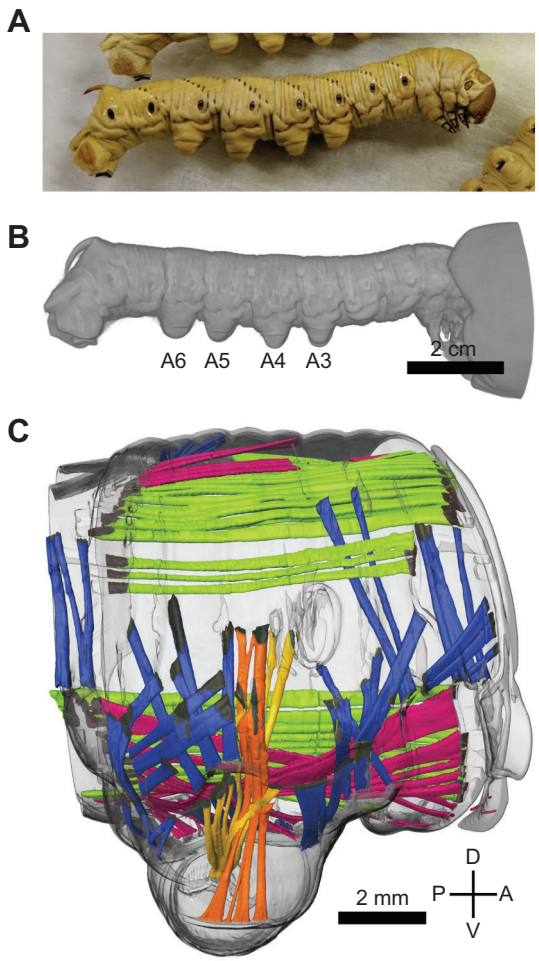

Fig. 1. Micro-computed tomography (micro-CT) of *Manduca sexta* larvae. (A) Fixed and stained fifth instar larvae were freeze dried and scanned with a micro-CT scanner. (B) Three-dimensional render of the unlabeled micro-CT scans, with segments A3–A6 indicated. (C) Labeled hemisegment. The cuticle is transparent to show the underlying muscles. Longitudinal fibers are shown in green, oblique fibers are in pink, radial fibers are in blue, and proleg-associated muscles (accessory planta retractor muscle, APRM; and principal planta retractor muscle, PPRM) are in orange and yellow, respectively. The dorso-ventral and anterior–posterior directions/vectors are indicated.

(Eaton, 1988; Hinton, 1955; Holst, 1934; Peterson, 1912; Snodgrass, 1961). This typically involves carefully removing tissues to access obscured anatomy and drawing or photographing relevant structures. Some reconstructions have also been attempted from histological sections (Lin et al., 2011). Both techniques distort the geometry of muscle, trachea, gut and cuticle from their intact configuration, which limits the resolution of the reconstruction.

In an attempt to circumvent these limitations, the internal anatomy of living *M. sexta* has been imaged using synchrotron-sourced high-energy X-rays (Simon et al., 2010b) but these studies are best for identifying physically distinct structures such as the trachea, while muscles and most other tissues are poorly resolved. A powerful alternative is to significantly enhance the resolution of soft tissues in dehydrated intact caterpillars using simple contrast agents and micro-computed tomography (micro-CT). Using this approach, it is possible to preserve the relative positions of the internal organs without significant distortion or damage, and features can be reconstructed with micrometer resolution.

In this paper, we describe using this technique to image the internal anatomy of *M. sexta* caterpillars. We show that muscles can be easily identified and that individual fibers can often be traced throughout their length in three dimensions. In addition to visualizing the origin and insertion sites of muscles throughout the body, it is possible to trace the direction and arrangement of fibers relative to one another, even when they are in close association. Our eventual goal is to describe the morphology of all the major muscles from undissected animals using X-ray micro-CT scanning. Here, we have focused on the detailed anatomy of an important muscle (PPRM) controlling proleg movements and show that it is composed of previously undescribed fibers that originate at different points on the body wall. These fibers are expected to affect the performance of the proleg during retraction. We also show that there are consistent differences in the size and number of these novel fibers in different body segments, suggesting that the anterior and posterior prolegs may play different functional roles. These additional fibers also provide mechanical complexity that might help to explain how prolegs can successfully release from a wide variety of substrates.

MATERIALS AND METHODS

Larvae preparation

Manduca sexta (Linnaeus 1763) larvae were raised from eggs to fifth instar on an artificial diet (n=6). The rearing incubator maintained a constant 27°C with a 17 h:7 h light:dark cycle (Bell and Joachim, 1978). Larvae (2nd day, fifth instar) were isolated from the colony and placed in 15 ml conical bottom centrifuge tubes (Corning, Corning, NY, USA). Whole animals were fixed for 1 week in Bouin's fixative (Sigma-Aldrich, St Louis, MO, USA) before being dehydrated in an ethanol series until 100% concentration was reached. The samples were stained in 2% iodine dissolved in ethanol solution for 1 week to enhance contrast of each tissue when they were scanned by micro-CT. After rinsing with 100% ethanol, they were transferred in liquidized *t*-butanol for 2–3 days and then freeze-dried. Samples were stored in a sealed container with desiccant until scanning to prevent distortion.

Micro-CT scanning

Samples were scanned using an X-ray micro-CT scanner (inspeXio SMX100CT, Shimazu, Kyoto, Japan) with an X-ray source operated at 100 kV and 40 µA. Resolution was prioritized to achieve ∼5–10 µm voxel size. Each animal was scanned several times to focus on whole-animal anatomy, individual segments and then highlighted areas of interest (plantar tip, spiracle, etc.).

Morphology reconstruction

Structures were manually reconstructed using the segmentation software Amira (v5.2, Visage Imaging Inc., Carlsbad, CA, USA) from DICOM image stacks. Muscle fibers were labeled by hand, slice by slice, creating a matrix of voxels that were convolved and smoothed to create a surface. Several parameters of the muscle fibers were collected from Amira (volume, attachment area, fiber number).

Comparisons of muscle size were made by calculating the attachment area of a given fiber or group of fibers on the body wall. This approach was used because computing the volume from fully labeled PPRM fibers from origin (on the body wall) to insertion (on the planta) was extremely labor intensive and it was occasionally difficult to distinguish abutting fibers near the planta. This method was validated by measuring both the muscle volume and attachment area for each PPRM fiber in a single body segment and showing they had a consistent relationship (see Results).

All muscle attachment area and fiber number data are expressed as means±s.e.m. Each muscle group was segmentally compared

Journal of Experimental Biology (2021) 224, jeb242508. doi:10.1242/jeb.242508

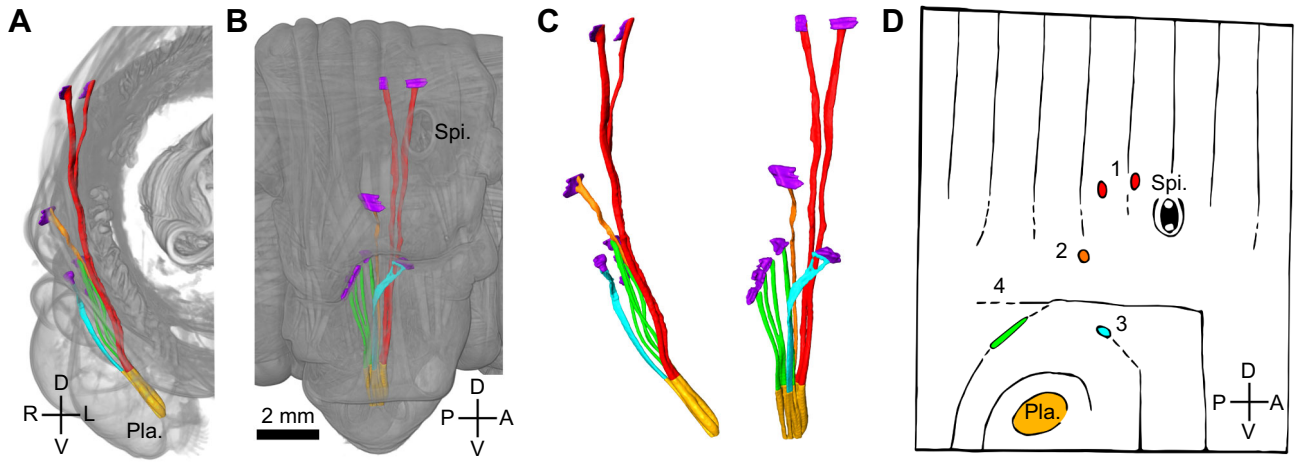

Fig. 2. Muscle insertion at the planta. (A) Cross-section showing the isolated proleg fibers. Fibers are colored based on their attachment site: $PPRM_{1,2,3,4}$ are in red, orange, teal and green, respectively. As the fibers near the planta, they become difficult to distinguish and have been colored yellow. (B) Sagittal view of the isolated proleg fibers. (C) Detail of the isolated muscle fibers, from cross-sectional (left) and sagittal (right) perspectives. (D) Cuticle map of PPRM attachments. Groups were created based on their attachment site. All fibers originate in the plantar tip of the proleg and extend to their respective number. $PPRM_1$ represents the canonical PPRM. Pla., planta; Spi., spiracle.

using a one-way analysis of variance (ANOVA). Statistics on fiber count and attachment areas were performed using JMP statistics software (v.15.2.0, SAS, Cary, NC, USA).

Histology

This protocol was adapted from Duch et al. (2000). Proleg muscle fibers were dissected with the planta tip intact and all fibers attached. The samples were fixed in 4% formalin in PBS and washed with PBS several times before incubation in phalloidin Alexa Fluor 488 to stain F-actin, followed by addition of DAPI solution to stain DNA. The fibers were then cut from the planta tip, spread on a glass slide and mounted in Fluoromount (catalog no. A12379, Sigma-Aldrich Chemical Co.). Slides were imaged using a Zeiss Axio Imager M1 microscope.

RESULTS

In general, the internal morphology of the larvae was well preserved, and all the major tissues were easily distinguished with high-resolution scanning (Fig. 1; Movie 1). In addition to the internal and external muscles and body wall, the nervous system, salivary glands, gut and fat body were distinguishable. Muscles were not broken or detached from their apodemes and their relative positions corresponded well with those described by dissection and histology (Eaton, 1988; Levine and Truman, 1985; Peterson, 1912; Weeks and Truman, 1985). In contrast to the results from dissection, the micro-CT scans produced images in which the arrangement of the muscle groups could be reconstructed in three dimensions and in the natural resting posture of the caterpillar. As an example unrelated to the proleg, longitudinal muscles inserting at the segment boundaries are arranged in two layers, the inner layer containing many large fibers running parallel to the body axis, while the outer layer consists of obliquely oriented fibers angled with respect to the body axis. In the reconstruction, it can been seen that some fibers pass between the different muscle groups to create an intricate network of muscles between the longitudinal fibers and the cuticle body wall (Fig. 1C).

A careful examination of muscles inserted at the planta revealed an unexpected diversity of fibers with different origins from those previously described (Fig. 2A–C; Movie 2). In addition to the fibers that originate close to the spiracle, several fibers were found that originate on the lateral body wall dorsal to the subcoxa–body fold (Fig. 2D).

Histology results

To confirm that these additional fibers are muscles, the planta tip was carefully dissected with its attached fibers and stained for actin and nuclei. The newly described fine fibers are extremely delicate and easily detached from their origins on the body wall (perhaps explaining why they have not been previously described), so they cannot be individually identified in isolated tissue. However, all the fibers inserted on the planta membrane (which includes the canonical $PPRM_1$ muscle fibers) were multinucleate cells that stained similarly, with actin striations organized into sarcomeres identifying them as striated muscles (Fig. 3B,C).

Canonical PPRM fibers

The PPRM has previously been described as a pair of fibers that originate posterior to the spiracle and insert on the planta membrane lateral to the crochets (Fig. 2). We refer to this fiber grouping as $PPRM_1$. These fibers were easily identifiable in the micro-CT scans and were consistent within a segment in terms of number and size (Fig. 4B,C). $PPRM_1$ made up 38.01±10.97% of the total fiber attachment area. The fiber attachment area did not vary between segments (one-way ANOVA, $F_{3,44}$=0.65, P=0.585). Fiber quantity for each proleg did not statistically differ from segment to segment ($F_{3,36}$=0.1304, P=0.9414).

Additional PPRM fibers

We found additional fibers inserted at the plantar tip and originating on the body wall in several locations (Fig. 2; Movie 2). These fibers were observed in all proleg-bearing segments (A3–A6) and their attachment sites and fiber numbers were consistent between animals and within a body segment. We identified these fiber groupings according to their attachment location as $PPRM_{2,3,4}$.

In general, the maximum force that can be developed by a muscle is proportional to its cross-sectional area but the various PPRM fibers differed in shape and overall size. Therefore, to compare the expected force contribution of different muscle groups, we measured the total cross-sectional area of both $PPRM_1$ fibers at

Journal of Experimental Biology (2021) 224, jeb242508. doi:10.1242/jeb.242508

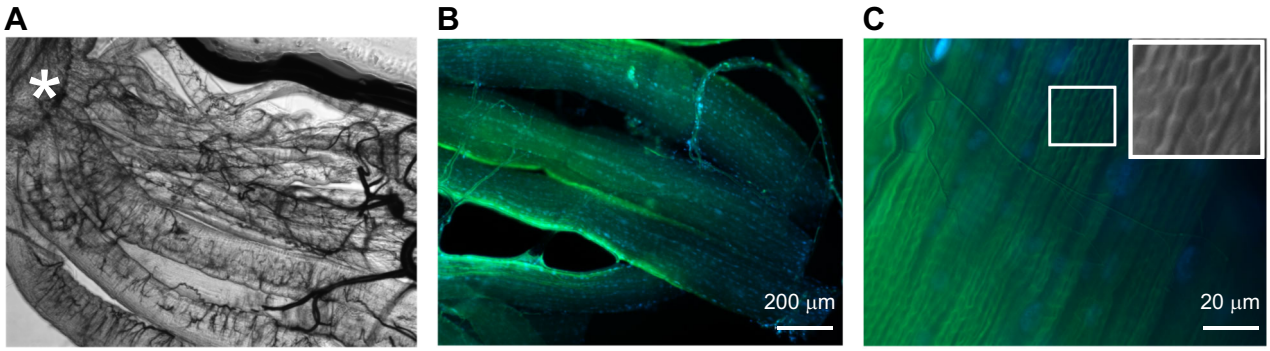

Fig. 3. Identification of planta fibers as muscle. (A) Brightfield image of fibers attached to the planta (asterisk). (B) Phalloidin (green; F-actin) and DAPI (blue; DNA) stain of excised proleg muscle fibers. Fibers excised from all proleg segments maintained a similar appearance and staining. (C) Individual proleg muscle fibers. Multinucleated cells with longitudinally aligned actin filaments can be clearly seen. This was true for all fibers inserting in the planta. Inset, expanded (2×) view of the boxed area in C, showing the fine detail of actin striations seen in all fibers. The banding striations in the actin filaments had an alignment mirroring that of muscle tissue.

50%, 70% and 90% of the muscle length from the planta to the cuticle attachment site and determined that the average cross-sectional area was directly proportional to the attachment area at the origin (Fig. 5; linear regression, $F_{1,30}$=22.18, P≤0.0001, R^2=0.425). The attachment area was then used to compare the predicted force contribution by each muscle group and to calculate their relative volume as attachment area×fiber length.

$PPRM_2$ fibers insert in the plantar tip, extend along the body wall and attach dorsal to the subcoxa–body fold (Figs 2 and 4A,B). The total attachment area did not vary between body segments (Fig. 4B, one-way ANOVA, $F_{3,44}$=0.11, P=0.95). This fiber group made up 10.30±2.96% of the total PPRM attachment area. Fiber quantity also did not significantly vary between segments (one-way ANOVA, $F_{3,36}$=1.09, P=0.3654).

$PPRM_3$ fibers attach to the plantar tip and extend along the proleg cuticle dorsally before wrapping around the posterior side of the APRM and inserting in the subcoxa–body fold on the anterior side. There were between one and three fibers on each side in all body segments and numbers were not significantly different between segments (one-way ANOVA, $F_{3,36}$=2.37, P=0.0869) (Fig. 4A,B). These fibers had the smallest attachment area (6.5±1.89% of the PPRM total), which did not vary between body segments (Fig. 4B; one-way ANOVA, $F_{3,44}$=1.85, P=0.152).

$PPRM_4$ fibers extend dorsally from the plantar tip and insert in the subcoxa–body fold on the posterior side. The attachment area of these fibers varied between body segments (one-way ANOVA, $F_{3,44}$=7.42, P=0.0004), as did the fiber number (one-way ANOVA, $F_{3,36}$=3.65, P=0.0215) (Fig. 4A,B). The attachment area of $PPRM_4$ was significantly higher in segment A6 than in segments A3 or A4 (Tukey's HSD, P=0.0004 and P=0.0039, respectively). The attachment area across other segments was not significantly different (Tukey's HSD, P>0.05). This group makes up a large portion of the total fiber attachment area, averaging 37.62±10.86% of total fiber attachment area.

DISCUSSION

Caterpillars provide an unusual opportunity for studying the neuromechanical control of soft-bodied locomotion. Other soft terrestrial invertebrates, such as worms and mollusks, have constant-volume hydrostatic skeletons, and blocks of antagonistic muscles that produce extension, shortening and bending (Kier, 2012). In contrast, insect larvae have an extensive internal gas-exchange system,

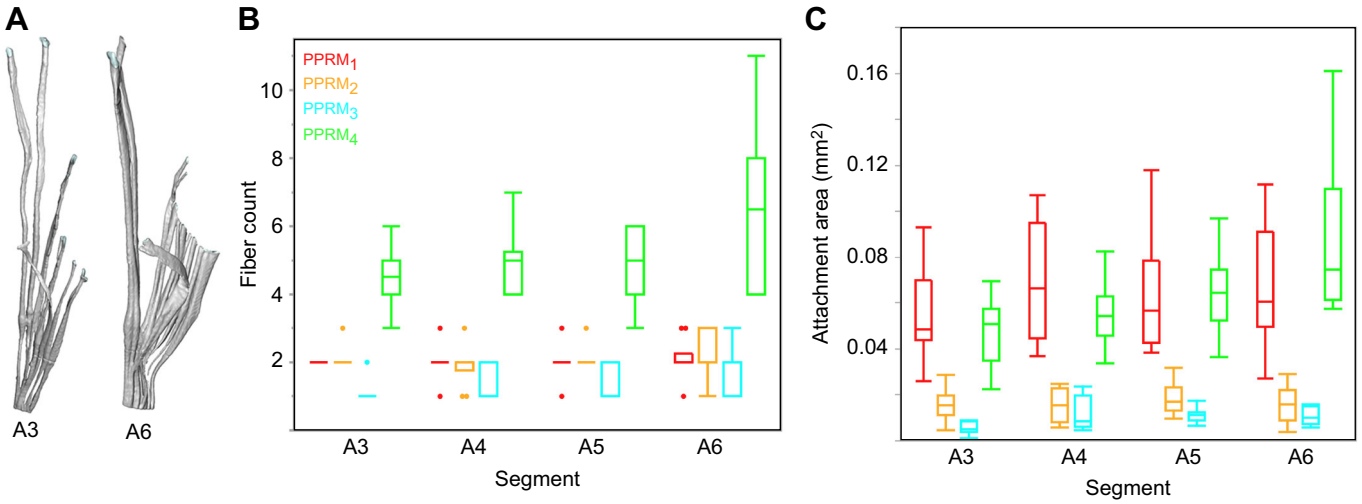

Fig. 4. Segmental differences. (A) Side by side comparison of PPRM fibers from anterior (A3) and posterior (A6) segments. (B) Fiber count by segment. Most fiber groups maintain fiber quantity across proleg-bearing segments. $PPRM_4$ shows a trend of increasing number of fibers but this was not statistically significant (one-way ANOVA, $F_{3,36}$=3.65, P=0.0215). (C) Attachment area by segment. Fiber attachment in each segment was only statistically different for $PPRM_4$ (one-way ANOVA, $F_{3,44}$=7.42, P=0.0004) (n=6 animals, 48 prolegs). Box plots indicate median (horizontal line), upper and lower quartiles (box) and 1.5× interquartile range.

Journal of Experimental Biology (2021) 224, jeb242508. doi:10.1242/jeb.242508

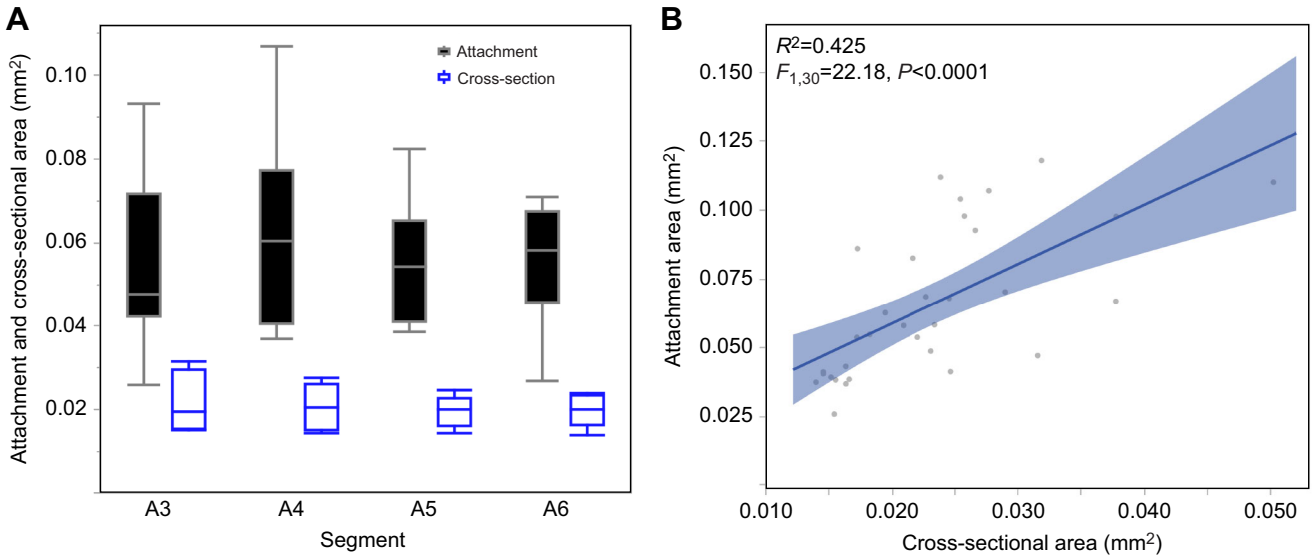

Fig. 5. Comparative muscle size measurements. (A) Averaged muscle–cuticle attachment area and cross-sectional area of $PPRM_1$ fibers as measured 50%, 70% and 90% from the planta insertion for segments A3–A6. (B) Comparison of $PPRM_1$ fiber cross-sectional area against attachment area at the origin, demonstrating that the attachment area is a suitable metric for approximating muscle size (n=4 animals, 32 prolegs).

consisting of air-filled tubes and sacs, that makes them compressible and limits internal fluid pressure (Lin et al., 2011). Furthermore, movements are mediated by many discrete and segmentally arranged muscles, each innervated by one or a few identifiable neurons. The activation of specific muscles can be monitored during natural behavior, thereby providing insight into the neural control strategies used by soft-bodied animals (Belanger and Trimmer, 2000; Berni, 2015; Gjorgjieva et al., 2013; Heckscher et al., 2012; Marescotti et al., 2018; Metallo and Trimmer, 2015; Mukherjee et al., 2018). However, larval muscles are precisely oriented in overlapping and complex arrangements that make it difficult to predict how each one affects movement. Previous descriptions of caterpillar morphology have produced detailed maps of muscles from flattened, dissected preparations (Barth, 1937; Forbes, 1914; Hinton, 1955; Libby, 1959; Peterson, 1912; Randall, 1968; Sivaprasad and Muralimohan, 2009; Tsujimura, 1983). These maps provide an excellent overview of the internal muscle complexity, but they are distorted and have limited spatial resolution.

The results described here, using micro-CT 3D scans of intact *M. sexta*, provide a detailed description of the internal anatomy in which the arrangement of tissues can be discerned with minimal distortion. Furthermore, the technique provides remarkable resolution with minimal damage and reveals structures that are difficult to see in traditional dissections. This method has revealed previously unknown proleg muscle fibers that are expected to change our current understanding of proleg grip release and movement control.

PPRM is a complex muscle

The new fibers were discovered by tracing the path of tissues attached to the planta tip. In addition to the well-known canonical PPRM fibers that extend to the lateral body wall close to the spiracle, we were surprised to find smaller bundles of fibers extending from the planta tip to several locations on the body wall. Based on brightfield imaging and histology staining, these proleg fibers were confirmed to be muscles with clearly delineated F-actin striations and well-organized multinucleated cells revealed by DAPI staining. In addition, excised fibers from each of the four proleg-bearing segments were carefully examined for differences in trachea supply and all were found to be heavily tracheated, which is typical for *M. sexta* larval muscle. Based on these findings we are confident that these discovered fibers are muscle fibers.

These additional fibers may help to explain some previously unexplained aspects of proleg retraction. It has been shown that grip release involves unhooking of the crochets and withdrawal of the planta away from the midline (Mukherjee et al., 2018; Weeks and Jacobs, 1987). Based on the known path of the $PPRM_1$ fibers, it was assumed that the rotation necessary to produce abduction resulted from the collapse of cuticular folds on the lower part of the proleg (Mezoff et al., 2004). However, the discovery of these additional PPRM fibers suggests that, instead of a singular force vector acting between the planta tip and upper body wall, forces are also applied much lower down the proleg and in a more lateral direction. This would be expected to rotate the planta away from the midline. It is currently not possible to record from these fibers directly during a movement, but we expect they will help to explain how a single motoneuron can affect proleg retraction under a wide variety of environmental conditions.

The neuromechanics of grip release

Animals with a rigid body and articulated limbs have finite degrees of freedom and can leverage that to simplify movement control in real time. Soft animals, such as tobacco hornworm larvae, do not have discrete joints and must rely on other methods of simplifying their control of a non-articulated body. This type of deferred complexity is referred to as morphological computation (Pfeifer and Bongard, 2006; Füchslin et al., 2013). A variety of strategies have been proposed, including distributed sensing, redundant actuation and structural or material adaptations. In these last two categories, the complex, non-linear and anisotropic properties of the tissues are thought to work as mechanical computers that automatically adjust to changing conditions, thereby reducing the computational load on the nervous system (Nakajima et al., 2018; Rieffel et al., 2008).

The proleg is expected to be a good model system for understanding the complex interactions between structural and

neural control (neuromechanics) in a soft animal. It is known that the motoneuron controlling the proleg retractor muscle does not change its overall firing rate very much, even when proleg loading is varied (Mukherjee et al., 2018). Instead, under high loading (for example, when the caterpillar is upside down), the principal planta retractor neuron fires at a low frequency in advance of retraction, which will pre-tension the muscle. This low-frequency stimulation is insufficient to collapse the planta or to initiate retraction but it is possible that it stiffens the newly discovered muscle fibers and changes the subsequent mechanical response of the proleg. It is currently difficult to predict how these additional fibers will alter movements of the proleg. We expect that they will shift the net force acting on the planta to a more lateral plane. This shift would allow for more optimal grip release from smaller diameter substrates as well as more stability when in vertical orientation as a result of the splaying of fibers. In addition to the muscles described here, we now have a highly detailed three-dimensional description of the proleg itself, which, when combined with the anisotropic constitutive properties of the body wall (Lin et al., 2009, 2011) and muscle (Paetsch et al., 2012), will allow us to develop a computational mechanical simulation of the proleg. This simulation will explore how the PPRM's complexity contributes to proleg adaptability and provide a better understanding of neuromechanical control of soft tissues in general.

Segmental specialization

The segmental specialization of these proleg muscles might suggest additional functions of the retractor muscles. Previous work measured the ground reaction forces (GRFs) of individual prolegs in the caterpillar while it was crawling (Lin and Trimmer, 2010a). While vertical GRF normal to the substrate remained consistent across segments A3, A4 and A6, horizontal GRF parallel to the substrate increased linearly from anterior to posterior segments. This mirrors the increase in fiber attachment area and fiber quantity in $PPRM_4$ muscles.

It is therefore possible that changes in fiber number and attachment area in $PPRM_4$ compensate for this increase in longitudinal tension in posterior segments. These segmental differences might also play a role during different stepping patterns (Metallo et al., 2020) or while crawling in different orientations (Metallo and Trimmer, 2015; Van Griethuijsen and Trimmer, 2014). During normal locomotion, it is common for multiple prolegs to be in swing phase at the same time. Therefore, the trailing proleg gripping the substrate experiences higher compressive forces and is pulled with more force by the longitudinal muscles in multiple anterior segments. This might explain why there are more retractor fibers in the posterior segments, helping to generate more tension and better distributing loads across the cuticle.

Another possibility is that the increased fiber number in segment A6 has a role in earlier instars. First instar larvae often grip the substrate with the terminal and A6 prolegs while holding their body elevated. At this stage, the A6 proleg is enlarged relative to the anterior segments so it is possible that the additional muscle fibers are important for providing a more stable attachment for newly emerged hatchlings.

Acknowledgements

The authors would like to thank J. C. Ludwig for assistance with the histology protocol and an anonymous reviewer for helpful suggestions on the functional role of the segmental fiber differences.

Competing interests

The authors declare no competing or financial interests.

Author contributions

Conceptualization: A.E.S.; Methodology: A.E.S., H.A.; Software: H.A.; Investigation: D.C.; Resources: H.A.; Data curation: D.C.; Writing - original draft: A.E.S.; Writing - review & editing: D.C., B.A.T.; Supervision: H.A., B.A.T.; Funding acquisition: B.A.T.

Funding

This work was supported by a National Science Foundation grant (IOS-1456471) to B.A.T., a National Science Foundation training grant (DGEIGERT-1144591) to B.A.T. and D.L.K., and Japan Science and Technology Agency, CREST (JPMJCR14D5) to H.A.

References

Barth, R. (1937). Muskulatur und Bewegungsart der Raupen. *Zool. Jahrb. Anat.* **62**, 507-566.

Belanger, J. H. and Trimmer, B. A. (2000). Combined kinematic and electromyographic analyses of proleg function during crawling by the caterpillar *Manduca sexta*. *J Comp Physiol A* **186**, 1031-1039. doi:10.1007/s003590000160

Belanger, J. H., Bender, K. J. and Trimmer, B. A. (2000). Context-dependency of a limb-withdrawal reflex in the caterpillar *Manduca sexta*. *J Comp Physiol [A]* **186**, 1041-1048. doi:10.1007/s003590000161

Bell, R. A. and Joachim, F. A. (1978). Techniques for rearing laboratory colonies of tobacco hornworms and pink bollworms. *Ann. Entomol. Soc. Am.* **69**, 365-373.

Berni, J. (2015). Genetic dissection of a regionally differentiated network for exploratory behavior in drosophila larvae. *Curr. Biol.* **25**, 1319-1326. doi:10.1016/j.cub.2015.03.023

Buschmann, T. and Trimmer, B. (2017). Bio-inspired robot locomotion. In *The Neurobiology of Motor Control: Fundamental Concepts and New Directions* (ed. S. L. Hooper and A. Büschges), pp. 443-472: Wiley-Blackwell.

Cox, S. C. (1989). The electrical and mechanical properties of the proleg retractor muscle of the chinese oak silkmoth larva. *Physiol. Entomol.* **14**, 265-272. doi:10.1111/j.1365-3032.1989.tb01092.x

Delp, S. L. and Loan, J. P. (2000). A computational framework for simulating and analyzing human and animal movement. *IEEE Computing in Science and Engineeriing* **2**, 46-55. doi:10.1109/5992.877394

Dembia, C. L., Bianco, N. A., Falisse, A., Hicks, J. L. and Delp, S. L. (2021). OpenSim Moco: Musculoskeletal optimal control. *PLoS Comput. Biol.* **16**, e1008493. doi:10.1371/journal.pcbi.1008493

Duch, C., Bayline, R. J. and Levine, R. B. (2000). Postembryonic development of the dorsal longitudinal flight muscle and its innervation in Manduca sexta. *J. Comp. Neurol.* **422**, 1-17. doi:10.1002/(SICI)1096-9861(20000619)422:1<1::AID-CNE1>3.0.CO;2-S

Eaton, J. L. (1988). *Lepidopteran Anatomy*. New York: John Wiley and Sons.

Forbes, W. T. M. (1914). A structural study of the caterpillars: iii, the somatic muscles. *Ann. Entomol. Soc. Am.* **7**, 109-124. doi:10.1093/aesa/7.2.109

Füchslin, R. M., Dzyakanchuk, A., Flumini, D., Hauser, H., Hunt, K. J., Luchsinger, R. H., Reller, B., Scheidegger, S. and Walker, R. (2013). Morphological computation and morphological control: steps toward a formal theory and applications. *Artif. Life* **19**, 9-34. doi:10.1162/ARTL_a_00079

Gjorgjieva, J., Berni, J., Evers, J. F. and Eglen, S. J. (2013). Neural circuits for peristaltic wave propagation in crawling Drosophila larvae: analysis and modeling. *Front. Comput. Neurosci.* **7**, 24. doi:10.3389/fncom.2013.00024

Gutfreund, Y., Flash, T., Fiorito, G. and Hochner, B. (1998). Patterns of arm muscle activation involved in octopus reaching movements. *J. Neurosci.* **18**, 5976-5987. doi:10.1523/JNEUROSCI.18-15-05976.1998

Hanassy, S., Botvinnik, A., Flash, T. and Hochner, B. (2015). Stereotypical reaching movements of the octopus involve both bend propagation and arm elongation. *Bioinspir. Biomim.* **10**, 035001. doi:10.1088/1748-3190/10/3/035001

Heckscher, E. S., Lockery, S. R. and Doe, C. Q. (2012). Characterization of Drosophila larval crawling at the level of organism, segment, and somatic body wall musculature. *J. Neurosci.* **32**, 12460-12471. doi:10.1523/JNEUROSCI.0222-12.2012

Hinton, H. E. (1955). On the structure, function and distribution of the prolegs of the panorpoidea, with a criticism of the Berlese-Imms theory. *Trans. R. Ent. Soc. Lond. B* **106**, 455-541. doi:10.1111/j.1365-2311.1955.tb01265.x

Holst, E. V. (1934). Motorische und tonischeErregung und ihr Bahnenverlauf bei Lepidopteranlarven. *Z. Vergl. Physiol.* **21**, 395-414.

Kier, W. M. (1988). The arrangement and function of molluscan muscle. *The Mollusca, Form and Function* **11**, 211-252. doi:10.1016/B978-0-12-751411-6.50016-3

Kier, W. M. (2012). The diversity of hydrostatic skeletons. *J. Exp. Biol.* **215**, 1247-1257. doi:10.1242/jeb.056549

Kier, W. M. and Smith, K. K. (1985). Tongues, tentacles and trunks: the biomechanics of movement in muscular-hydrostats. *Zool. J. Linn. Soc.* **83**, 307-324. doi:10.1111/j.1096-3642.1985.tb01178.x

Kier, W. M. and Stella, M. P. (2007). The arrangement and function of octopus arm musculature and connective tissue. *J. Morphol.* **268**, 831-843. doi:10.1002/jmor.10548

Levine, R. B. and Truman, J. W. (1985). Dendritic reorganization of abdominal motoneurons during metamorphosis of the moth, *Manduca sexta*. *J. Neurosci.* **5**, 2424-2431. doi:10.1523/JNEUROSCI.05-09-02424.1985
Levy, G., Flash, T. and Hochner, B. (2015). Arm coordination in octopus crawling involves unique motor control strategies. *Curr. Biol.* **25**, 1195-1200. doi:10.1016/j.cub.2015.02.064
Levy, G., Nesher, N., Zullo, L. and Hochner, B. (2017). Motor control in soft-bodied animals. In *The Oxford Handbook of Invertebrate Neurobiology* (ed. J. H. Byrne). Oxford University Press.
Libby, J. L. (1959). The nervous system of certain abdominal segments of the cecropia larva (Lepidoptera; Saturniidae). *Ann. Entomol. Soc. Am.* **52**, 469-480. doi:10.1093/aesa/52.4.469
Lin, H.-T. and Trimmer, B. A. (2010a). The substrate as a skeleton: ground reaction forces from a soft-bodied legged animal. *J. Exp. Biol.* **213**, 1133-1142. doi:10.1242/jeb.037796
Lin, H. T. and Trimmer, B. A. (2010b). Caterpillars use the substrate as their external skeleton: a behavior confirmation. *Commun. Integr. Biol.* **3**, 471-474. doi:10.4161/cib.3.5.12560
Lin, H. T., Dorfmann, A. L. and Trimmer, B. A. (2009). Soft-cuticle biomechanics: a constitutive model of anisotropy for caterpillar integument. *J. Theor. Biol.* **256**, 447-457. doi:10.1016/j.jtbi.2008.10.018
Lin, H. T., Slate, D. J., Paetsch, C. R., Dorfmann, A. L. and Trimmer, B. A. (2011). Scaling of caterpillar body properties and its biomechanical implications for the use of a hydrostatic skeleton. *J. Exp. Biol.* **214**, 1194-1204. doi:10.1242/jeb.051029
Marescotti, M., Lagogiannis, K., Webb, B., Davies, R. W. and Armstrong, J. D. (2018). Monitoring brain activity and behaviour in freely moving Drosophila larvae using bioluminescence. *Sci. Rep.* **8**, 9246. doi:10.1038/s41598-018-27043-7
Matzner, H., Gutfreund, Y. and Hochner, B. (2000). Neuromuscular system of the flexible arm of the octopus: physiological characterization. *J. Neurophysiol.* **83**, 1315-1328. doi:10.1152/jn.2000.83.3.1315
Metallo, C. and Trimmer, B. A. (2015). Orientation-dependent changes in single motor neuron activity during adaptive soft-bodied locomotion. *Brain Behav. Evol.* **85**, 47-62. doi:10.1159/000369372
Metallo, C., Mukherjee, R. and Trimmer, B. A. (2020). Stepping pattern changes in the caterpillar *Manduca sexta*: the effects of orientation and substrate. *J. Exp. Biol.* **223**, jeb220319. doi:10.1242/jeb.220319
Mezoff, S., Papastathis, N., Takesian, A. and Trimmer, B. A. (2004). The biomechanical and neural control of hydrostatic limb movements in Manduca sexta. *J. Exp. Biol.* **207**, 3043-3053. doi:10.1242/jeb.01136
Mukherjee, R., Vaughan, S. and Trimmer, B. A. (2018). The neuromechanics of proleg grip release. *J. Exp. Biol.* **221**, jeb173856. doi:10.1242/jeb.173856
Nakajima, K., Hauser, H., Li, T. and Pfeifer, R. (2018). Exploiting the dynamics of soft materials for machine learning. *Soft Robotics* **5**, 339-347. doi:10.1089/soro.2017.0075
Nishikawa, K. C., Kier, W. M. and Smith, K. K. (1999). Morphology and mechanics of tongue movement in the African pig-nosed frog Hemisus marmoratum: a muscular hydrostatic model. *J. Exp. Biol.* **202**, 771-780. doi:10.1242/jeb.202.7.771
Paetsch, C., Trimmer, B. A. and Dorfmann, A. (2012). A constitutive model for active-passive transition of muscle fibers. *Int. J. Non-Linear Mech.* **47**, 377-387. doi:10.1016/j.ijnonlinmec.2011.09.024
Peterson, A. (1912). Anatomy of the tomato-worm larva, Protoparce carolina. *Ann. Entomol. Soc. Am.* **5**, 246-272. doi:10.1093/aesa/5.3.246
Pfeifer, R. and Bongard, J. (2006). *How The Body Shapes The Way We Think: A New View Of Intelligence*: MIT press.
Quillin, K. J. (1998). Ontogenetic scaling of hydrostatic skeletons: geometric, static stress and dynamic stress scaling of the earthworm *Lumbricus terrestris*. *J. Exp. Biol.* **201**, 1871-1883. doi:10.1242/jeb.201.12.1871
Randall, W. C. (1968). Anatomical changes in the neuromuscular complex of the proleg of *Galleria mellonella* (L.) (Lepidoptera: Pyralidiadae) during metamorphosis. *J. Morphol.* **125**, 105-127. doi:10.1002/jmor.1051250106
Richter, J. N., Hochner, B. and Kuba, M. J. (2015). Octopus arm movements under constrained conditions: adaptation, modification and plasticity of motor primitives. *J. Exp. Biol.* **218**, 1069-1076. doi:10.1242/jeb.115915
Rieffel, J., Trimmer, B. and Lipson, H. (2008). Mechanism as mind: what tensegrities and caterpillars can teach us about soft robotics. In *Artificial Life XI: Proceedings of the Eleventh International Conference on the Simulation and Synthesis of Living Systems*, Vol. 11 (ed. J. N. S. Bullock, R. Watson and M. A. Bedau), pp. 506-512. Winchester, UK: MIT Press, Cambridge, MA.
Sandstrom, D. J. and Weeks, J. C. (1996). Novel dual innervation of a larval proleg muscle by two similar motoneurons in the tobacco hornworm Manduca sexta. *J. Exp. Biol.* **199**, 775-791. doi:10.1242/jeb.199.4.775
Simon, M. A., Fusillo, S. J., Colman, K. and Trimmer, B. A. (2010a). Motor patterns associated with crawling in a soft-bodied arthropod. *J. Exp. Biol.* **213**, 2303-2309. doi:10.1242/jeb.039206
Simon, M. A., Woods, W. A., , Jr, Serebrenik, Y. V., Simon, S. M., van Griethuijsen, L. I., Socha, J. J., Lee, W. K. and Trimmer, B. A. (2010b). Visceral-locomotory pistoning in crawling caterpillars. *Curr. Biol.* **20**, 1458-1463. doi:10.1016/j.cub.2010.06.059
Sivaprasad, S. and Muralimohan, P. (2009). Neuromuscular systems in the fifth instar larva of silkworm Bombyx mori (Lepidoptera: Bombycidae): II- Abdominal musculature and its innervation. *J. Appl. Nat. Sci.* **1**, 210-226. doi:10.31018/jans.v1i2.60
Smith, K. K. and Kier, W. M. (1989). Trunks, tongues, and tentacles - moving with skeletons of muscle. *Am. Sci.* **77**, 29-35.
Snodgrass, R. E. (1961). The caterpillar and the butterfly. *Smithsonian Miscellaneous Collections* **143**, 51.
Sumbre, G., Fiorito, G., Flash, T. and Hochner, B. (2005). Neurobiology: Motor control of flexible octopus arms. *Nature* **433**, 595-596. doi:10.1038/433595a
Taylor, H. M. and Truman, J. W. (1974). Metamorphosis of the abdominal ganglia of the tobacco hornworm, *Manduca sexta*. *J. Comp. Physiol.* **90**, 367-388. doi:10.1007/BF00694177
Thelen, D. G., Anderson, F. C. and Delp, S. L. (2003). Generating dynamic simulations of movement using computed muscle control. *J. Biomech.* **36**, 321-328. doi:10.1016/S0021-9290(02)00432-3
Trimmer, B. and Issberner, J. (2007). Kinematics of soft-bodied, legged locomotion in *Manduca sexta* larvae. *Biol. Bull.* **212**, 130-142. doi:10.2307/25066590
Trimmer, B. A. and Lin, H.-T. (2014). Bone-free: soft mechanics for adaptive locomotion. *Integr. Comp. Biol.* **54**, 1122-1135. doi:10.1093/icb/icu076
Tsujimura, H. (1983). Anatomy of external structure and musculature of abdominal segments in the larva of the lepidopteran *Pieris rapae crucivora*. *J. Morphol.* **177**, 191-203. doi:10.1002/jmor.1051770206
Van Griethuijsen, L. and Trimmer, B. (2014). Locomotion in caterpillars. *Biol. Rev.* **89**, 656-670. doi:10.1111/brv.12073
Weeks, J. C. and Jacobs, G. A. (1987). A reflex behavior mediated by monosynaptic connections between hair afferents and motoneurons in the larval tobacco hornworm, *Manduca sexta*. *J. Comp. Physiol. A* **160**, 315-329. doi:10.1007/BF00613021
Weeks, J. C. and Truman, J. W. (1985). Independent steroid control of the fates of motoneurons and their muscles during insect metamorphosis. *J. Neurosci.* **5**, 2290-2300. doi:10.1523/JNEUROSCI.05-08-02290.1985
Yekutieli, Y., Sagiv-Zohar, R., Aharonov, R., Engel, Y., Hochner, B. and Flash, T. (2005). Dynamic model of the octopus arm. I. Biomechanics of the octopus reaching movement. *J. Neurophysiol.* **94**, 1443-1458. doi:10.1152/jn.00684.2004